Polymer Journal, Vol. 27, No. 12, pp 1230—1238 (1995)

Crystal Transition Mechanisms in Poly(tetramethylene succinate)†

Yasushi ICHIKAWA,†† Junichiro WASHIYAMA, Yoshihiro MOTEKI, Keiichi NOGUCHI,* and Kenji OKUYAMA*

Bionolle Project, Kawasaki Plastics Laboratory, Showa Denko K.K., 3–2, Chidori-cho, Kawasaki-ku, Kawasaki 210, Japan
**Faculty of Technology, Tokyo University of Agriculture and Technology, Koganei, Tokyo 184, Japan*

(Received July 14, 1995)

ABSTRACT: Poly(tetramethylene succinate) (PTMS) showed a crystal transition between the α ($T_7GT\bar{G}$) and β (T_{10}) form under the strain and relaxation conditions, where T, G, and $\bar{G}$ denoted *trans*, *gauche*, and *minus gauche*, respectively. We have investigated the mechanisms of this crystal transition by FT-IR and X-ray diffraction. In the FT-IR, the absorbance peaks at 920 cm^{-1} and 955 cm^{-1}, corresponding to the α form, started decreasing at strain of $\varepsilon \sim 8\%$, while the absorbance at 977 cm^{-1}, corresponding to the β form, appeared at $\varepsilon \sim 8\%$, then increased with strain. In addition, the isobestic point was observed at 965 cm^{-1}, indicating that the crystal transition occurred only between the α and β form, where no amorphous part contributed. In the X-ray diffraction, the meridional reflection of α (at $2\theta = 25.1°$) started decreasing at $\varepsilon \sim 8\%$. In addition, the reflection of β (at $2\theta = 22.5°$) appeared at $\varepsilon \sim 8\%$, then increased with ε. These FT-IR and X-ray results were thus consistent with each other. The molar fraction of the β form, χ_β, was determined as a function of stress, σ, by X-ray. The χ_β showed a drastic increase at a critical value of $\sigma = 140$ MPa. It was hence concluded that the thermodynamic first-order phase transition was the operative mechanism of the transition. Such a crystal transition mechanism had been also reported in poly(butylene terephthalate) (PBT). The free energy difference between the α and β form, ΔG, was determined to be $\Delta G \sim 1.6$ (kJ mol^{-1} of monomer unit), being close to the reported value of $\Delta G \sim 1.4$ (kJ mol^{-1} of monomer unit) for the crystal transition in PBT. The stress–strain curve was measured. The σ increased with ε when $\varepsilon < 8\%$, then remained approximately constant up to $\varepsilon \sim 16\%$, followed by the second increase for $\varepsilon > 16\%$. Such a stress–strain characteristics could be explained in terms of the crystal transition.

KEY WORDS Poly(tetramethylene succinate) / Crystal Transition Mechanism / Crystal Structure / X-Ray Diffraction / FT-IR / Stress–Strain Curve /

As represented by poly(tetramethylene succinate) (PTMS), which is crystalline polymer, biodegradable aliphatic polyesters have received a great attention from industry, particularly from the ecological viewpoint.[1,2] Mechanical properties of such crystalline polymers, in general, depend strongly on their crystal structure as well as on the crystallinity of the polymers.[3] Crystal structures can be controlled by pressure, temperature and strain. Recently, we have discovered such crystal modifications in PTMS (α and β form): the transition occurred under application or removal of strain, and the β form appeared under strain.[4] The conformations of the two forms were ($T_7GT\bar{G}$)[5] and (T_{10})[4] for the α and β form, respectively: the conformational modification occurred in the tetramethylene units.

Strain induced crystal modifications have

† Part of this work was presented at the International Symposium on Fiber Science and Technology on October 26—28, 1994 in Yokohama, Japan.

†† To whom correspondence should be addressed.

been reported in many polymers. In poly(butylene terephthalate) (PBT), for instance, two kinds of crystal modifications (α and β form) have been reported:[6-15] the β form appeared under strain. Yokouchi *et al.*[9a] determined the crystal structures of the α and β form in PBT and showed that the transition occurred between $\bar{G}\ \bar{G}\ TGG$ (α form) and $T\bar{S}\ TST$ (β form) in the tetramethylene units, where T, G, $\bar{G}$, S, and $\bar{S}$ and denoted *trans*, *gauche*, *minus gauche*, *skew*, and *minus skew*, respectively. Concurrently, Hall *et al.*[9b] reported a different conformation of the β form of PBT to be $TTTTT$. Siesler[10] and Tashiro *et al.*[11] found an isobestic point in FT-IR during the transition, indicating that the crystal transition took place only between the α and β forms. Roebuck *et al.*[12] studied the stability of the β form under residual stress. Further studies have been conducted by NMR[13] as well as by the measurements of mechanical[14] or dynamic mechanical properties.[15] Besides in PBT, such strain induced crystal modifications were reported in Keratin[16,17] and in poly(ethylene oxide) (PEO),[18] as well as in a series of poly(butylene terephthalate)–poly(tetramethylene oxide) block copolymers.[19-21]

The crystal transition mechanisms were well investigated in PBT by Tashiro *et al.*[11] and by Roebuck *et al.*[12] as well as in Keratin.[16,17] In these investigations, two different models were proposed for the transition mechanisms. The first one was a kinetic model, where the concentration of each crystal form was determined by the "reaction" rate from one to the other; *i.e.*, the free energy barrier associated with the transition dictated the fraction of each crystal form. Such a kinetic model accounted well for the crystal transition behavior in Keratin.[16] The second one was the thermodynamic first-order phase transition model. As opposed to the former model, the fraction of each crystal during the transition is determined by the free energy difference, ΔG, between equilibrium states of the two crystal phases. According to this model, fraction of the β form showed a discontinuous change at a certain value of stress, in addition to the existence of a plateau in a stress–strain curve. Such a mechanism was observed typically in PBT,[11] its copolymers[19-21] and poly(ethylene oxide) (PEO).[18]

Despite many investigations on the crystal modification and transition in PBT, few works have been reported on PTMS, only the crystal structure (α-form) in a uniaxially oriented fiber[5] and in a single crystal[22] as well as the existence of a crystal modification[4] were reported in PTMS. This paper principally focused on the crystal transition mechanisms in PTMS with a special emphasis on the comparison to those observed in PBT.

EXPERIMENTAL

Materials

The polymer material used in this study was poly(tetramethylene succinate) (PTMS), so called Bionolle (grade 1001). PTMS was supplied in commercial pellets form from Showa Highpolymer Co., Ltd.; no further purification was made on the polymer. The weight average molecular weight was determined to be 1.6×10^5 by size exclusion chromatography with poly(methylmethacrylate) standards. The melting (T_m) and glass transition temperatures (T_g) were measured to be 114°C and -32°C, respectively (by DSC). The crystallinity, X_c, of the fiber was $X_c \sim 30\%$ (by X-ray and DSC).

Sample Preparation

Uniaxially oriented fibers were fabricated by melt spinning at 200°C, followed by the drawing up to 10 times at room temperature, which were then annealed at 80°C in vacuum under a constant length. The diameter of the fibers was 500 μm. These fiber specimens were utilized in the following X-ray studies. Film specimens were also prepared under the identical thermal conditions for the FT-IR studies.

X-Ray Measurements

Nickel-filtered Cu-K_α radiation operated at 40 kV and 30 mA was used throughout this investigation. Wide angle X-ray diffractions were measured at room temperature under various strains between 0 and 20%, where the stepwise strains were applied to the fiber with the interval of 4%. The diffraction curve for each strain was obtained 30 minutes after the application of the strain: we have confirmed the stress to reach an equilibrium value and remained constant ($\sim$85% of the initial stress) under this condition. The near meridional reflection of the ($\bar{1}03$) of the α form was measured by the 2θ scan method at $\phi = 5°$, and that of the β form was obtained by the $\theta/2\theta$ symmetric scan method. X-ray fiber photographs were also taken for both the original and strained (by 14%) fibers by means of a cylindrical camera (diameter of 100 mm) as reported previously.[4] In addition, small angle X-ray diffraction was measured to determine the long period for detail analyses.

FT-IR Measurements

FT-IR spectra of PTMS were obtained at room temperature under stepwise strains as described in the above. We mainly focused on the absorbance peaks at 920 and 955 cm^{-1} (for the α form) and the peak at 977 cm^{-1} (for the β form): these peaks disappeared in a molten state.

Stress–Strain Curves

Stress–strain curves were measured by means of a tensilon (Toyo Baldwin Co., Ltd.: model UTM-IV) at a strain rate of 5% min^{-1} at room temperature.

RESULTS AND DISCUSSION

FT-IR Spectra

The FT-IR spectra of PTMS under various strains are shown in Figure 1. The absorbance peaks at 955 and 920 cm^{-1} start decreasing at strain of $\varepsilon \sim 8\%$, while the peak at 977 cm^{-1} appears at $\varepsilon \sim 8\%$. These observations thus indicate that the peaks at 955 and 920 cm^{-1} correspond to the α form crystal, and the peak at 977 cm^{-1} is assigned to the β form. It is worthwhile to point out that the spectra have an isobestic point at 965 cm^{-1}. According to Siesler[10] and Tashiro *et al.*,[11] the existence of such an isobestic point indicates that the crystal transition occurs only between the α form and the β form, where no amorphous part is transformed into crystal. It is thus possible to evaluate the molar fraction of the β form, χ_β, as a function of ε,[11] where we employ the peak at 806 cm^{-1}, which is not altered by strain, as an internal standard.

As shown in Figure 2, χ_β, starts increasing at $\varepsilon \sim 8\%$ and shows a reversible change with respect to the application or removal of strain. Tashiro *et al.*[11] reported that an appreciable amount of the β form remained after the relaxation of the strain, so called hysteresis, while PTMS shows no such hysteresis. This difference may arise from the residual strain (or stress) involved in the specimens.[11,12] Since the T_g of PBT and PTMS are 40°C and -32°C, respectively, the structural relaxation in PTMS would be faster than that in PBT. It should be noted that $\chi_\beta \neq 0$ even at $\varepsilon = 0$, which is also observed in PBT. The contribution from

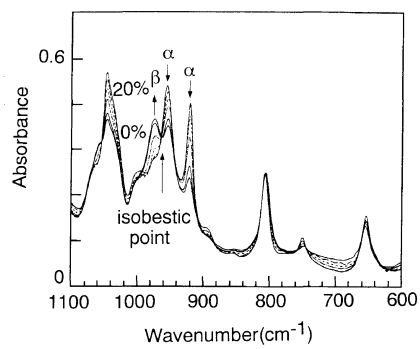

Figure 1. FT-IR spectra under various strains (0—20%) are shown. Note that the absorbance peaks at 955 and 920 cm^{-1} start increasing at $\varepsilon = 8\%$ (broken line), while the peak at 977 cm^{-1} appears at $\varepsilon = 8\%$ then increases with strain. The existence of the isobestic point at 965 cm^{-1} should also be noted.

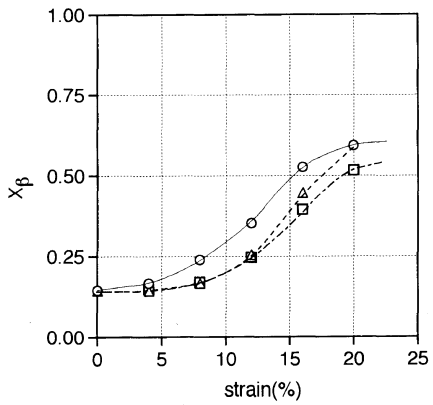

Figure 2. The χ_β is plotted as a function of strain. Note that χ_β starts increasing at $\varepsilon \sim 8\%$: these changes are reversible ○, 1st load; △, unload; □, 2nd load.

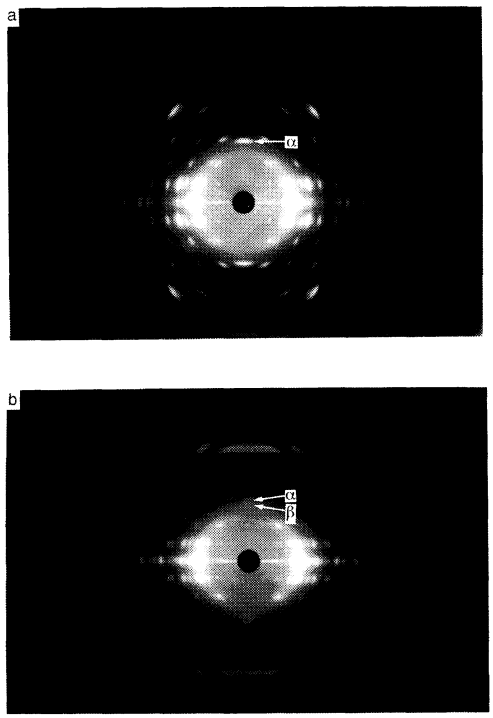

Figure 3. The X-ray fiber photographs are shown: (a) for the α form ($\varepsilon = 0\%$), (b) for the β form ($\varepsilon = 14\%$).

an amorphous phase also appears in the absorbance, resulting in such a non-zero χ_β even at $\varepsilon = 0$.[11] In order to eliminate such contribution, a "normalized" χ'_β has been introduced for further quantitative analyses.[11] Such a contribution from the amorphous phase would more or less introduce ambiguity to the quantitative interpretation of the data. We thus employ X-ray diffraction method hereafter for more quantitative analyses, where only the signals from crystal phase can be extracted.

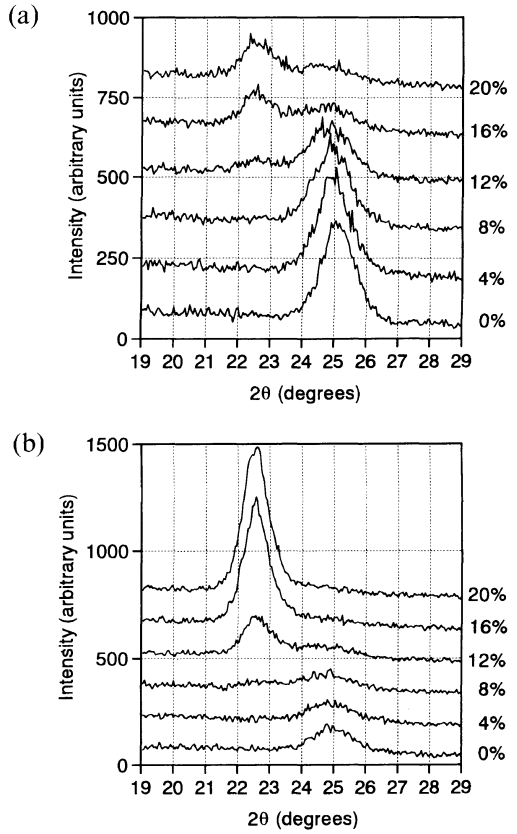

Figure 4. The meridional reflection curves are shown. The reflection peaks at $2\theta = 25.1°$ and $2\theta = 22.5°$ correspond to (a) the α and (b) β reflections, respectively. Note that the a reflection starts decreasing at $\varepsilon \sim 8\%$, while the β reflection appears at $\varepsilon \sim 8\%$ then increases with strain.

X-Ray Diffraction

The X-ray fiber photographs for the α ($\varepsilon = 0$) and β ($\varepsilon = 14\%$) forms are shown in Figure 3. The reflection spots indicated by the arrows are used for the later analyses. The meridional reflection curves under various strains are plotted in Figure 4. The easily distinguishable reflection peaks at $2\theta = 25.1°$ and $2\theta = 22.5°$ correspond to the third layer lines of the α ($\bar{1}03$)

and β forms, respectively. It should be noted that the intensity of the reflection at $2\theta=25.1°$ starts decreasing at $\varepsilon\sim8\%$ (see Figure 4a), while the reflection at $2\theta=22.5°$ appears at $\varepsilon\sim8\%$ then increases with ε (see Figure 4b). In addition, the change is reversible with respect to the repeated application and removal of stain. These observations are consistent with the FT-IR results. It is found, in the equatorial reflections, that the intensity of the α (020) peak at $2\theta=19.4°$ starts decreasing at $\varepsilon\sim8\%$, which is similar to the case of the α ($\bar{1}03$) reflection, however, no clear reflection from the β form is observed.

The above two meridional reflections were thus used for the determination of χ_β. The details of the procedure are described in below. First, the integrated intensity of the a reflection, I_α, is plotted with respect to the intensity of the β reflection, I_β, for each strain in Figure 5, where the data points fall on a single straight line with a slope of $1/a$ (Note that the a is negative.). Then χ_β is calculated *via* eq 1.[14,23]

$$\chi_\beta = I_\beta/(I_\beta - aI_\alpha) \qquad (1)$$

The χ_β is thereby plotted as a function of ε in Figure 6a. The χ_β starts increasing at $\varepsilon\sim8\%$ and shows a drastic increase with increasing ε, then, almost saturates at $\varepsilon\sim16\%$. These observations indicate that the transition occurs between $\varepsilon\sim8\%$ and $\varepsilon\sim16\%$, consistent with the FT-IR results (see Figure 2), although, in the FT-IR, the transition is not so drastic. The transition behaviors observed by FT-IR and X-ray in this study are thus essentially the same as those observed in PBT.[11] In order to evaluate the critical stress of the transition, the χ_β *vs.* ε plot is converted into χ_β *vs.* σ (see Figure 6b), from the relationship between ε and an equilibrium value of σ at each ε. Details will be discussed in the next section. In addition, the crystal modulus of the α form was determined to be 13 GPa through the conventional method.[25,26]

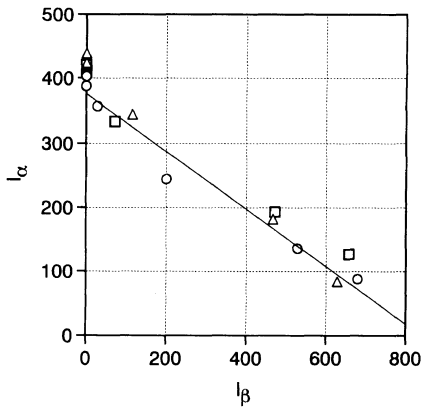

Figure 5. The integrated intensity of the reflection at $2\theta=25.1°$, I_α, is plotted with respect to that at $2\theta=22.5°$, I_β. Note that the data points fall on a single straight line. ○, 1st load; △, unload; □, 2nd load.

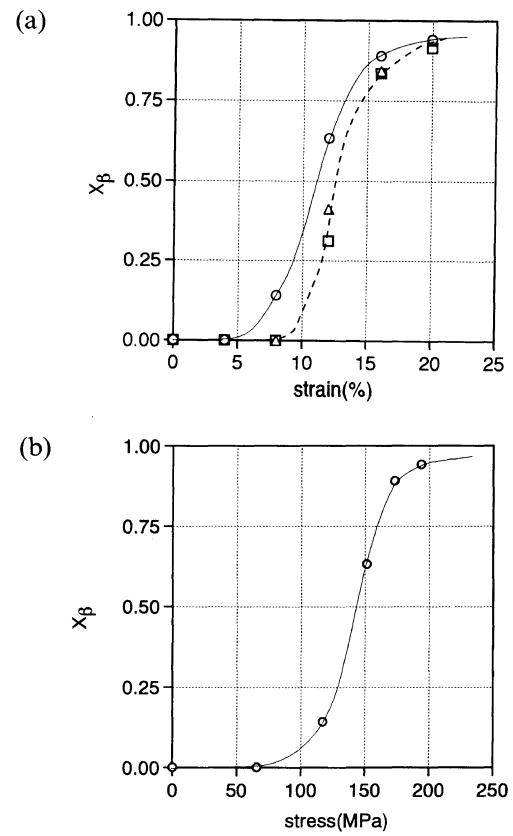

Figure 6. The χ_β, obtained by X-ray, is plotted as a function of (a) strain and (b) stress. Note that χ_β starts increasing at $\varepsilon\sim8\%$ or $\sigma\sim140$ MPa. ○, 1st load; △, unload; □, 2nd load.

Crystal Transition Mechanisms

Two different models have been proposed for the crystal transition mechanisms: one is the kinetic model, the other is the thermodynamic first-order phase transition model. In the former model, χ_α and χ_β are determined by the reaction rate, *i.e.*, the free energy barrier, between α and β; and consequently, the plot $\ln(\chi_\beta/\chi_\alpha)$ *vs.* σ should fall on a single straight line.[11,16] In the latter model, χ_β should show a discontinuous jump at a certain value of σ ($=\sigma^*$: critical stress). These two kinds of plots therefore give a critical examination for the models. In addition, the existence of a plateau in the stress–strain curve will give a further confirmation of the latter model.[11,14] In the case of PTMS, the $\ln(\chi_\beta/\chi_\alpha)$ *vs.* σ does not fall on a single straight line at all, ruling out the kinetic model. On the other hand, the χ_β shows a drastic increase at nearly a constant value of σ ($\sim$140 MPa) (see Figure 6b). These observations indicate that the crystal transition mechanism in PTMS is the thermodynamic first-order phase transition rather than the kinetic one, as reported in PBT.[11] The crystal transitions in both PTMS and PBT take place in the tetramethylene units. We would thus expect that the crystal transition in PTMS occurs through the same transition mechanism as in PBT, consistent with our observations.

The Critical Stress

The critical stress, σ^*, is determined based on the definition that $\chi_\beta=0.5$ at $\sigma=\sigma^*$, and we thereby obtain σ^* to be $\sigma^*\sim140$ MPa in PTMS and $\sigma^*=75$ MPa in PBT. Since the transition mechanism is the thermodynamic first-order phase transition, σ^* is given by[11]:

$$\sigma^*=\Delta G/[A_\alpha(L_\beta-L_\alpha)] \qquad (2)$$

where ΔG and A_α denote the difference in the free energy between the α and β form per monomer unit and the cross sectional area of the α form, respectively. The values of such parameters for PTMS and PBT, as well as the conformation change in tetramethylene units, are summarized in Table I. It should be noted that the ΔG of PTMS [$\sim$1.6 (kJ mol^{-1} of monomer unit)] is close to that of PBT [$\sim$1.4 (kJ mol^{-1} of monomer unit)].[11] Since both PTMS and PBT have the same crystal transition mechanism in the same units (tetramethylene),[4,9] the contribution from the conformation change would be a principal factor of ΔG. In the fourth column, the data for PEO are also listed[18]: $\Delta G\sim0.97$ (kJ mol^{-1} of monomer unit). This number seems to be somewhat smaller than that for PTMS or PBT. The conformation change upon transition occurs in the ethylene oxide units in PEO, as opposed to PTMS and PBT. This comparison may result in such a different number of ΔG. For further quantitative interpretation, detail knowledge of the energy states in both crystal forms is necessary, and this point is deserved for the future projects.

Mechanical Property

The stress–strain curve in PTMS is shown in Figure 7. The apparent modulus (*i.e.*, slope) starts decreasing at $\varepsilon\sim8\%$ then reaches at an approximately constant value, followed by the second increase beyond $\varepsilon\sim16\%$. Such stress–strain characteristics can be explained in terms of the crystal transition as discussed in the previous sections. No β form is present when $\varepsilon<\sim8\%$, the stress–strain characteristic is thus dictated by X_c and the modulus of the α form. Similarly, in the case of $\varepsilon>\sim16\%$, almost all crystals are β form, so that the stress–strain characteristic is dictated by the

Table I. Crystal transition parameters for PTMS, PBT, and PEO

Materials	PTMS	PBT	PEO
α Form	*TGTḠT*	*ḠḠTGG*	*TTG*
β Form	*TTTTT*	*TTTTT*	*TTT*
A_α/Å^2	19.7	22.44	21.45
$L_\beta-L_\alpha$/Å	0.96	1.36	0.78
σ^*/MPa	140	75	97
ΔG/kJ mol^{-1}	1.6	1.4	0.97

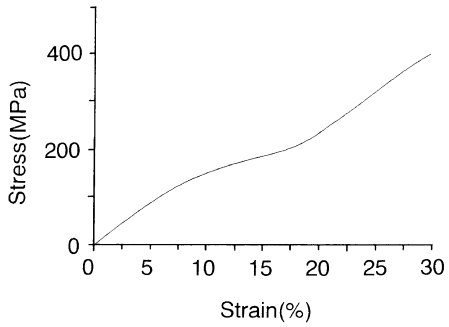

Figure 7. Stress–strain curve is shown.

modulus of the β form. As opposed to these two cases, crystal transition occurs in the range of $8\% < \varepsilon < 16\%$, the stress thus does not increase so much with ε, since the transition would take place under an approximately constant stress. These observations in Figure 8 are thus consistent with the FT-IR and X-ray results. Similar stress–strain characteristics have also been reported and explained in terms of a crystal transition in PBT,[11,14] Keratin[16,17] and in PEO.[18]

In the transition regime, crystals in the α form turn into the β form under an approximately constant stress of σ^*. The increase in the strain during the transition arises from the increase in the fiber identity periods from the α to the β form,[11] where the deformation in the amorphous region is assumed to remain constant. The magnitude of the transition regime, $\Delta\varepsilon \equiv \varepsilon_e - \varepsilon_i$, is thus given by eq 3 based on a series model.

$$\Delta\varepsilon_{calc} = X\{[(L_\beta - L_\alpha)/L_\alpha] - (\sigma^*/E_\alpha)\} \quad (3)$$

where ε_i and ε_e denote the strains at the initial and end of the transition, respectively. The $\Delta\varepsilon_{calc}$ and $\Delta\varepsilon_{obs}$ denote the estimated and observed values for $\Delta\varepsilon$, respectively. L_α and L_β represent the fiber periods of the α and β form, respectively. $X = L_{cr}/L$, where L_{cr} and L denote the crystal size and the long period of the a form along the fiber axis, respectively. E_α denotes the crystal modulus of the α form. The first term in the right hand side of eq 3 represents the strain arising from the difference in the fiber identity period of each crystal forms. The second term represents the strain in crystals (α form) in the initiation of the transition. In the case of PBT, $\Delta\varepsilon_{calc} \sim 9\%$ with $X = 0.8$, $L_\alpha = 11.59$ Å, $L_\beta = 12.95$ Å, $\sigma^* = 75$ MPa, and $E_\alpha = 13.5$ GPa, which is close to the observed value of $\Delta\varepsilon_{obs} \sim 10\%$.[11] In the case of PEO, the strain is obtained to be $\Delta e_{calc} \sim 24\%$, with $X = 0.9$, $L_\alpha = 2.78$ Å, $L_\beta = 3.56$ Å (per monomer unit), $\sigma^* = 97$ MPa and $E_\alpha = 10.0$ GPa, which is close to the observed number of $\Delta\varepsilon_{obs} \sim 26\%$.[18] In PTMS, $\Delta\varepsilon_{calc} \sim 6.5\%$ with $X = 0.8$, $L_\alpha = 10.90$ Å, $L_\beta = 11.90$ Å,[4] $\sigma^* = 140$ MPa, and $E_\alpha = 13$ GPa, which is also close to $\Delta\varepsilon_{obs} \sim 8\%$. These correlations thus indicate that the magnitude of the strain in the transition regime, $\Delta\varepsilon$, is determined by eq 3.

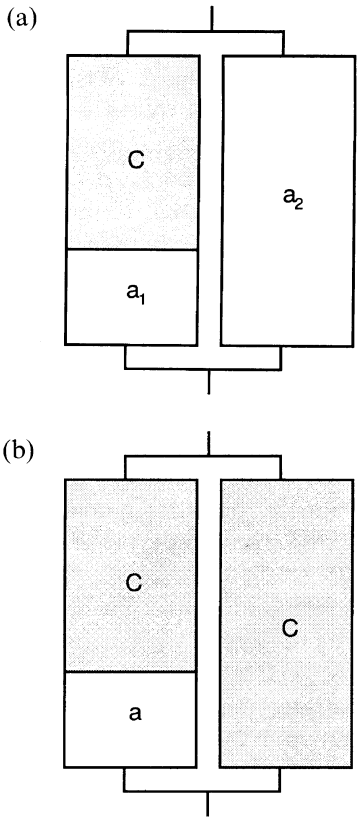

Figure 8. The Takayanagi models for (a) PTMS and PBT and (b) PEO are illustrated.

It should be pointed out that in PTMS, as

well as in PBT, the plateau is vague ε in the transition regime, while a distinct pateau in the transition regime has been reported in PEO. We expect this comparison will arise from the inhomogeneous stress distribution in the polymer.[26] According to the principle of the Takayanagi model,[27] for instance, two kinds of amorphous components can be defined: one is a series component connected to crystals (a_1), the other one is a parallel component surrounding the crystals (a_2) as illustrated in Figure 8a. The stress in the a_1 component remains constant even in the transition regime, while that in the a_2 component increases with strain, resulting in a slight increase in the total stress in the transition regime. PTMS and PBT would contain a_1 component, since the X_c's ($X_c \sim 0.3$—0.4) are much smaller than that in PEO ($X_c > 0.8$). On the other hand, the model corresponding to PEO will be very close to that for ultra-high modulus polyethylene, where amorphous is surrounded by crystal[28] (see Figure 8b), since the X_c is extremely high. We would thus expect that such a comparison in the transition regime arises from the stress in the parallel amorphous component.

CONCLUSIONS

We have investigated the crystal transition mechanisms between the α and β form in poly(tetramethylene succinate) (PTMS) by using FT-IR and X-ray diffraction. In the FT-IR, the absorbance peaks for the α form (920 and 955 cm^{-1}) started decreasing at strain of $\varepsilon \sim 8\%$, while the absorbance of the β form (977 cm^{-1}), appeared at $\varepsilon \sim 8\%$, then increased with strain. In addition, the isobestic point was observed at 965 cm^{-1}.

The molar fraction of the β form, χ_β, was determined as a function of stress, σ, by X-ray, and the χ_β showed a drastic increase at $\sigma \sim 140$ MPa, consistent with the FT-IR results. These observations indicated that the thermodynamic first-order phase transition was the operative mechanism of the transition. Such a crystal transition mechanism was also reported in poly(butylene terephthalate) (PBT). The free energy difference between the α and β form, ΔG, was then estimated to be $\Delta G \sim 1.6$ (kJ/mol^{-1} of monomer unit), being comparable to the value $\Delta G \sim 1.4$ for PBT.

The stress–strain curve was measured, where the σ increased with ε when $\varepsilon < 8\%$, then remained approximately constant up to $\varepsilon \sim 16\%$, followed by the second increase for $\varepsilon > 16\%$. These observations were consistent with the X-ray and FT-IR results, and the stress–strain characteristics could be explained in terms of the crystal transition.

Acknowledgement. The authors acknowledge the fruitful discussions and strong encouragement on this work by Prof. K. Tashiro of Osaka University.

REFERENCES

1. Y. Yokota, R. Ishioka, and N. Watanabe, Abstracts, "3rd International Scientific Workshop on Biodegradable Plastics and Polymers," Nov. 1993, Osaka Japan, p 96.
2. M. Nishioka, T. Tuzuki, Y. Wanajyo, F. Oonami, and T. Horiuchi, Abstracts, 3rd International Scientific Workshop on Biodegradable Plastics and Polymers," Nov. 1993, Osaka Japan, p 97.
3. L. E. Nielsen, "Mechanical Properties of Polymers and Composites," Marcel Dekker Inc., New York, N.Y., 1975.
4. Y. Ichikawa, J. Suzuki, J. Washiyama, Y. Moteki, K. Noguchi, and K. Okuyama, *Polymer*, **35**, 3338 (1994).
5. Y. Chatani, R. Hasegawa, and H. A. Tadokoro, *Polymer Prepr. Jpn.*, **20**, 420 (1971).
6. C. A. Boyle and J. R. Overton, *Bull. Am. Phys. Soc.*, **19**, 352 (1974).
7. R. Jakeways, M. A. Wilding, I. M. Ward, I. H. Hall, I. J. Desborough, and M. G. Pass, *J. Polym. Sci., Polym. Phys. Ed.*, **13**, 799.
8. F. M. Lu and J. E. Spruiell, *J. Appl. Polym. Sci.*, **21**, 1595.
9a. M. Yokouchi, Y. Sakakibara, Y. Chatani, H. Tadokoro, T. Tanaka, and K. Yoda, *Macromolecules*, **9**, 266, (1976).
9b. I. H. Hall and M. G. Pass, *Polymer*, **17**, 807 (1976).
10. H. W. Siesler, *J. Polym. Sci., Polym. Lett. Ed.*, **17**, 453 (1979).
11. K. Tashiro, Y. Nakai, M. Kobayashi, and H.

Tadokoro, *Macromolecules*, **13**, 137 (1980).
12. J. Roebuck, R. Jakeways, and I. M. Ward, *Polymer*, **33**, 227 (1992).
13. B. C. Perry, J. L. Koenig, and J. B. Lando, *Macromolecules*, **20**, 422 (1987).
14. M. G. Brereton, G. R. Davis, R. Jakeways, T. Smith, and I. M. Ward, *Polymer*, **19**, 17 (1978).
15. G. R. Davis, T. Smith, and I. M. Ward, *Polymer*, **21**, 221 (1980).
16. M. Feughelman, *J. Polym. Sci.*, **10**, 1937 (1966).
17. A. Ciferri, *Trans. Faraday Soc.*, **59**, 562 (1963).
18. K. Tashiro and H. Tadokoro, *Rep. Prog. Polym. Phys. Jpn.*, **21**, 417 (1978).
19. K. Tashiro, M. Hiramatsu, T. Ii, M. Kobayashi, and H. Tadokoro, *Seni Gakkaishi (Japan)*, **42**, T-597 (1986).
20. K. Tashiro, M. Hiramatsu, T. Ii, M. Kobayashi, and H. Tadokoro, *Seni Gakkaishi (Japan)*, **42**, T-65^9 (1986).
21. E. Dobrovolny-Marand, S. L. Hsu, and C. K. Shih, *Macromolecules*, **20**, 1022 (1987).
22. K. J. Ihn, E. S. Yoo, and S. S. Im, *Macromolecules*, **28**, 2460 (1995).
23. R. Jakeways, T. Smith, I. M. Ward, and M. A. Wilding, *J. Polym. Sci., Polym. Phys. Ed.*, **14**, 41 (1976).
24. I. Sakurada, Y. Nukushina, and T. Ito, *Kobunshi Kagaku*, **19**, 285 (1962).
25. I. Sakurada, T. Ito, and K. Nakamae, *J. Polym. Sci. C*, **15**, 75 (1966).
26. K. Tashiro, G. Wu, and M. Kobayashi, *Polymer*, **29**, 1768 (1988).
27. M. Takayanagi, K. Imada, and T. Kajiyama, *J. Polym. Sci. C*, **15**, 263 (1966).
28. J. Clements, R. Jakeways, and I. M. Ward, *Polymer*, **19**, 639 (1978).